nature geoscience

ARTICLES

PUBLISHED ONLINE: 28 JUNE 2009 | DOI: 10.1038/NGEO554

# Southward movement of the Pacific intertropical convergence zone AD 1400–1850

Julian P. Sachs[1]*, Dirk Sachse[1†], Rienk H. Smittenberg[1†], Zhaohui Zhang[1†], David S. Battisti[2] and Stjepko Golubic[3]

**Tropical rainfall patterns control the subsistence lifestyle of more than one billion people. Seasonal changes in these rainfall patterns are associated with changes in the position of the intertropical convergence zone, which is characterized by deep convection causing heavy rainfall near 10° N in boreal summer and 3° N in boreal winter. Dynamic controls on the position of the intertropical convergence zone are debated, but palaeoclimatic evidence from continental Asia, Africa and the Americas suggests that it has shifted substantially during the past millennium, reaching its southernmost position some time during the Little Ice Age (AD 1400–1850). However, without records from the meteorological core of the intertropical convergence zone in the Pacific Ocean, quantitative constraints on its position are lacking. Here we report microbiological, molecular and hydrogen isotopic evidence from lake sediments in the Northern Line Islands, Galápagos and Palau indicating that the Pacific intertropical convergence zone was south of its modern position for most of the past millennium, by as much as 500 km during the Little Ice Age. A colder Northern Hemisphere at that time, possibly resulting from lower solar irradiance, may have driven the intertropical convergence zone south. We conclude that small changes in Earth's radiation budget may profoundly affect tropical rainfall.**

The primary features of Northern Hemisphere climate during the past 1,200 years were the Little Ice Age (LIA), the culmination of a 600-year-long cooling trend that began in AD 1250 and the subsequent warming since AD 1850 (ref. 1). Evidence for the LIA comes primarily from tree rings and mountain glaciers in Northern Hemisphere middle latitudes[1]. Relatively little is known about the tropical ocean at that time, even though massive fluxes of latent heat, moisture and momentum originate in the tropics, and theory and models indicate that changes in tropical Pacific climate are propagated globally[2]. Most tropical records that resolve the past 1,200 years are from on or near continents[3–14] where seasonal heating and topographic effects significantly influence climate. Records that are removed from monsoonal and continental influences, that span the past millennium and that have decadal or better resolution are virtually non-existent for several reasons. Changes in the spatial difference of tropical sea surface temperature (SST) of just a few tenths of a degree create large changes in climatological precipitation[15], but such SST changes are too small for current palaeotemperature proxies to discern. Sediment accumulation rates in the tropical Pacific Ocean are generally too low to resolve the past 1 kyr. Surface ocean temperature and salinity signals can be difficult to separate from $^{18}O/^{16}O$ measurements in calcium carbonate fossils. In addition, it is inherently difficult to deduce past precipitation patterns from a massive region of ocean. We circumvent these issues by using microbiological, molecular and isotopic indicators of rainfall from rapidly accumulating sediments in lakes on the Northern Line Islands, Palau and the Galápagos (Fig. 1), of which the mid-ocean locations span the tropical Pacific Ocean and the zonal extent of the modern intertropical convergence zone (ITCZ). In so doing, we are able to demonstrate large basin-wide shifts in the precipitation patterns of the tropical Pacific during the past millennium.

## Evidence from the central Pacific Ocean

Washington Island (Teraina, 4°43′ N, 160°25′ W) and Christmas Island (Kiritimati, 1°52′ N, 157°20′ W) have remarkably different climates for islands separated by 280 km of latitude in the central Pacific Ocean. Washington Island receives 2,903 mm rain $yr^{-1}$ owing to its perennial location under the ITCZ (Fig. 1) and contains a freshwater lake and peat bogs[16,17]. Christmas Island receives 896 mm rain $yr^{-1}$ but has net precipitation minus evaporation of $-2$ mm $d^{-1}$ because the ITCZ is virtually always to its north[17], resulting in hundreds of hypersaline evaporative ponds.

Today, Washington Lake is 3.7 m deep and contains 9.3 m of sediment[17] deposited during the past 3,200 years (see Supplementary Table S1) that consists of four distinct units (Fig. 2a). Unit I (0–112 cm) sediment is unconsolidated brown organic-rich freshwater gyttja (Fig. 2b) with abundant beige fecal pellets and the remains of the freshwater green algae *Tetraedron minimum* (A in Fig. 2c) and *Scenedesmus quadricauda* (B in Fig. 2d). Modern radiocarbon ($^{14}C$) ages indicate extensive bioturbation in this uppermost sedimentary unit (Fig. 2a, Supplementary Table S1).

Unit II (112–230 cm) is a gelatinous red–orange microbial mat (Fig. 2e) with abundant rod-shaped cyanobacteria from the *Aphanothece* morphotype (Fig. 2f) known to produce prodigious quantities of exopolysaccharide gel. Ages for these sediments will be reported on two slightly different chronologies owing to insufficient evidence favouring one over the other (Fig. 3, Supplementary Table S1). Deposition of unit II began about AD 1400 or 1410 (from here: AD 1405) and ended about AD 1560 or 1640 (from here:

[1]School of Oceanography, University of Washington, Seattle, Washington 98195, USA, [2]Department of Atmospheric Sciences, University of Washington, Seattle, Washington 98195, USA, [3]Biological Science Center, Boston University, Boston, Massachusetts 02215, USA. †Present addresses: DFG-Leibniz Center for Surface Process and Climate Studies, Institut für Geowissenschaften, Universität Potsdam, 14476 Potsdam, Germany (D.S.); Geological Institute, ETH Zürich, 8092 Zürich, Switzerland (R.H.S.); Department of Earth Sciences, Nanjing University, Nanjing, 210093, China (Z.Z.).
*e-mail: jsachs@u.washington.edu.

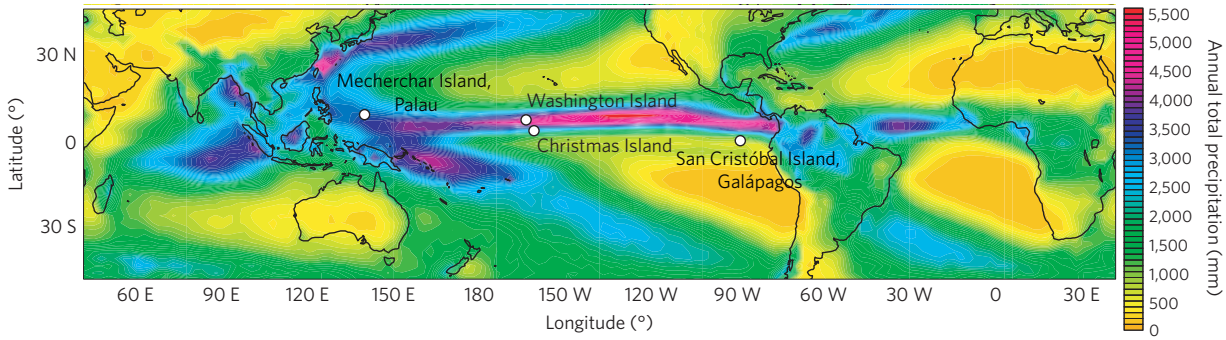


**Figure 1 | Map of mean annual precipitation in the tropical Pacific with our sampling locations shown.** The band of heavy precipitation indicates the ITCZ. Data from ref. 44.

AD 1560/1640). The upper 40 cm (112–152 cm; Unit IIa) contains occasional beige fecal pellets (Fig. 2e) containing *S. quadricauda* (B in Fig. 2g) as observed in Unit I (Fig. 2b), implying that changing environmental conditions had begun to support the growth of freshwater algae in lake surface water.

Unit III (230–571 cm; about AD 1405–760) is a red–orange microbial mat with a leather-like texture (Fig. 2h), interbedded with well-preserved 0.5–1 mm layers that were composed predominantly of empty sheaths of the filamentous cyanobacterium *Leptolyngbya* sp. (D in Fig. 2i) and remnants of globular colony-forming cyanobacteria of the *Entophysalis* morphotype (E Fig. 2j). The transition between units III and IV is marked by a 0.5-cm-thick layer of plant debris, suggesting a change from a semi-closed lagoon to the present-day closed basin, perhaps caused by a storm or tsunami. Unit IV (571 cm to core end at 730 cm, about 540 BC–AD 760), consisted primarily of authigenic fine-grained calcium carbonate (Fig. 2a). Core WL2 ended at 730 cm but in parallel core WL1 the unit extended to bedrock at 930 cm, dated 980 BC ± 210 (see Supplementary Table S1).

The most remarkable feature and an unambiguous indicator of a severe change in the climate of Washington Island is the lithologic transition at 112 cm from pure red microbial mat to modern tropical gyttja (Fig. 2a). Below we use microbiology and hydrogen isotope ratios in lipids from Unit II–III sediments to conclude that, unlike today, Washington Island was arid from about AD 760 until at least AD 1560/1640, and perhaps until the late eighteenth century.

Although microbial mats are found in a variety of extreme environments, it is hypersalinity that favours the development of thick mat sequences by limiting species richness and grazers[18,19]. A hypersaline Washington Lake would require an excess of evaporation over precipitation characteristic of arid settings such as Christmas Island today. Indeed, Unit II–III sediments are strikingly similar to modern microbial mats growing in hypersaline ponds on Christmas Island (Fig. 2k–n). Filamentous *Leptolyngbya* (F in Fig. 2l,m) and coccoid *Aphanothece* cyanobacteria (G in Fig. 2m) in Christmas Island lake F6 (117 psu salinity) microbial mats were similar to microbial structures in Unit II sediments from Washington Lake (D in Fig. 2i and C in Fig. 2f, respectively). Moreover, the extensive accumulations of empty, compacted *Leptolyngbya* sheaths (D in Fig. 2n) and *Entophysalis* colonies (E in Fig. 2n) embedded within the orange gelatinous material below the living mat in lake F6 on Christmas Island appear identical to the empty sheaths (D in Fig. 2i) and colonies (E in Fig. 2j) in Unit III sediments from Washington Lake, respectively, indicating that Unit II–III sediments from Washington Island were deposited in a hypersaline pond such as those found on Christmas Island today.

The microscopic observations of an arid climate on Washington Island are corroborated by high hydrogen isotope ratios ($\delta$D) of lipids in the Unit II–III microbial mat sediments (see Supplementary Table S5) that are similar to those values observed in microbial mats from the modern hypersaline ponds on Christmas Island[20]. There the Rayleigh distillation mechanism that normally causes deuterium enrichment in residual water as evaporation proceeds is opposed by the isotopic exchange between deuterium-depleted water vapour in the marine atmospheric boundary layer and the hygroscopic surface of hypersaline ponds[21]. As a result, water $\delta$D values in Christmas Island ponds spanned just 10.4‰, varying from 5.4 to 15.8‰, over a 110 psu salinity range from 40 to 150 psu (ref. 20). Yet $\delta$D values of lipids (as total lipid extracts, TLEs) from microbial mats spanned 106‰, varying between −190 and −84‰, and were closely correlated with salinity, owing to a decrease in D/H fractionation between lipids and source water as salinity increases[20]. TLE $\delta$D values can therefore be used as a salinity indicator in hypersaline environments such as those at Christmas Island (see also Supplementary Discussion).

Applying the TLE $\delta$D versus salinity relationship from Christmas Island to the $\delta$D values in Unit II–III sediments from Washington Lake, which were between −170 and −116‰ (see Supplementary Table S5), implies salinities of 52–126 psu (Fig. 4a) during the microbial mat deposition. Although we assume that water $\delta$D values in Washington Lake from about AD 760–1560/1640 were close to the range of values observed in Christmas Island ponds today, even a 10‰ deviation from the extremes of that range would alter our salinity estimates by only 14 psu. Furthermore, temporal variations in microbial or algal species and the lipids they produced during the deposition of Unit II–III sediments in Washington Lake are assumed to be within the spatial variation encountered on Christmas Island from which the empirical salinity calibration was derived.

From about 980–1380 (if no pre-aged carbon was in the lake) or AD 1050–1390 (if 15% of the carbon in the lake came from the surrounding ocean) (Fig. 3), TLE $\delta$D values of −170 to −148‰ indicate that salinities ranged from 52 to 80 psu (Fig. 4a, Supplementary Table S5). They then increased rapidly to 126 psu ($\delta$D = −116‰) around AD 1420, at the base of Unit II, when the dominant genus of cyanobacteria changed from *Leptolyngbya* (Fig. 2i) to extremely salt-tolerant *Aphanothece* (Fig. 2f) that flourish in salinities up to 210 psu (ref. 22). From AD 1420 to 1560/1640, salinity declined to 86 psu ($\delta$D = −145‰) (Fig. 4a), accelerating around AD 1550 or 1630 when the surface of Washington Lake must have been intermittently fresh, as demonstrated by *S. quadricauda* in fecal pellets from Unit IIa (Fig. 2e,g).

In summary, Washington Island was arid from AD 980 to 1560 or AD 1050 to 1640 when TLE $\delta$D values imply that Washington Lake had a salinity of 52–126 psu (Fig. 4a). The presence of salt-tolerant microbes in Unit II–III sediments such as those in hypersaline ponds on Christmas Island today extends the inference of aridity on Washington Island from 1560/1640 back to about AD 760 (Fig. 2).

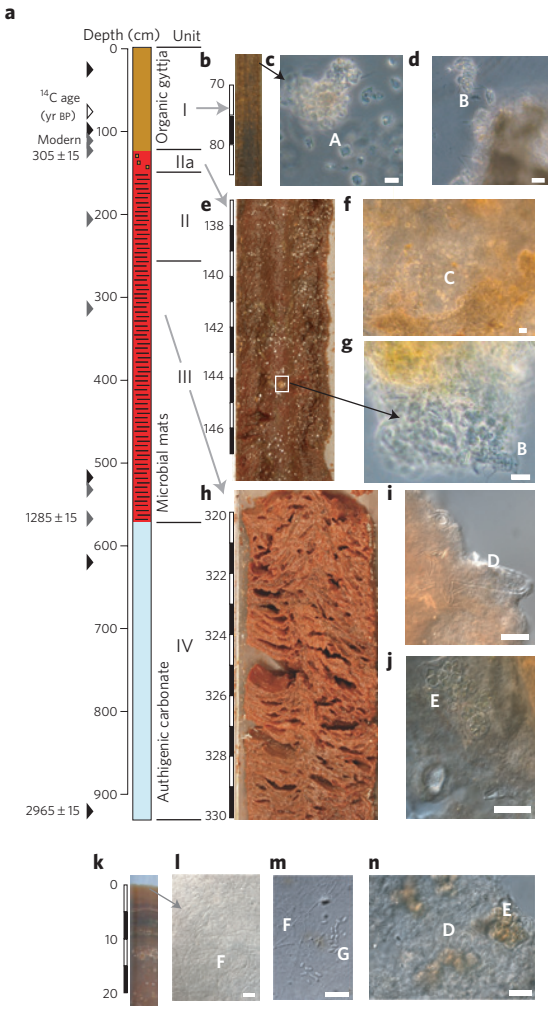


**Figure 2 | Sediment features from Washington Lake and Christmas Island lake F6. a–j**, Washington Lake sediment images. **a**, Composite core schematic and lithological units of Washington Lake sediment. The shaded triangles indicate radiocarbon dates in different cores (see Supplementary Table S1). **b**, Unit I sediment from 66–87 cm. **c**, Fecal pellets and freshwater green algae *T. minimum* (A). **d**, Freshwater green algae *S. quadricauda* (B). **e**, Unit IIa sediment from 137–148 cm consisting of gelatinous red microbial mat material with an embedded fecal pellet highlighted. **f**, Remnants of coccoid *Aphanothece* morphotype cyanobacteria (C) at 156 cm. **g**, Fecal pellet with remnants of *S. quadricauda* (B). **h**, Unit III sediment from 319.5–330 cm indicating red, leathery microbial mat layers. **i**, Empty sheaths of filamentous *Leptolyngbya* morphotype cyanobacteria (D) at 330 cm. **j**, Remains of colonial *Entophysalis* morphotype cyanobacteria (E) at 330 cm. **k–n**, Christmas Island lake F6 sediment images. **k**, Surface core from Christmas Island lake F6. **l**, Living sheath-forming filamentous *Leptolyngbya* morphotype cyanobacteria (F) at 0–1 cm. **m**, Living *Leptolyngbya* morphotype (F) and coccoid *Aphanothece* morphotype cyanobacteria (G) at 0–1 cm. **n**, Remains of the colonial *Entophysalis* morphoptype cyanobacteria (E) and consolidated empty sheaths derived from *Leptolyngbya* morphotype cyanobacteria (D) at 13–14 cm. The vertical scale bars are in centimetres composite core depth; the white bars represent 10 μm.

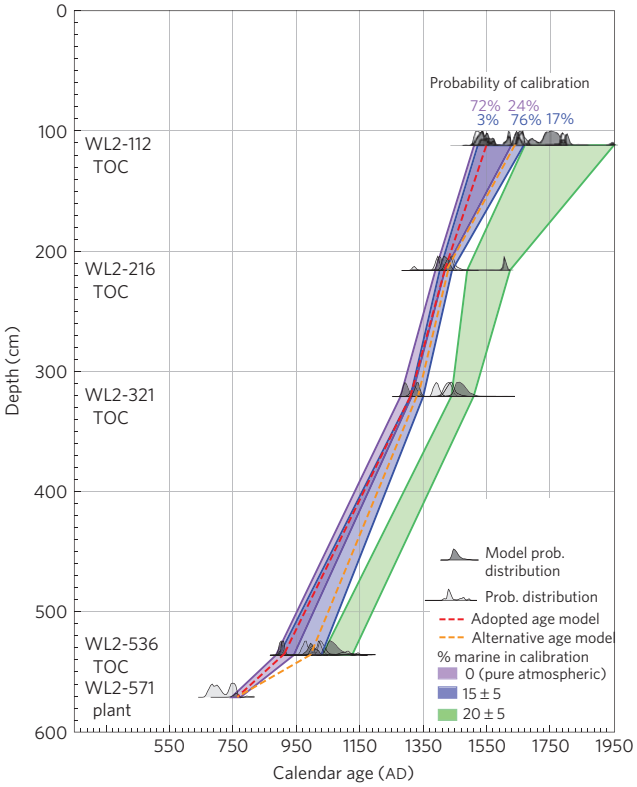


**Figure 3 | Age–depth models for Washington Lake sediment.** Probability distributions for the five radiocarbon calibrations from core WL2, unit II–III samples, with respectively 0 (purple), 15 (blue) and 20% (green) marine contribution to a mixed atmospheric–marine calibration curve. TOC: total organic carbon. The shaded areas represent the 1$\sigma$ probability age ranges constructed with the OxCal software[38] by interpolating between $^{14}$C age control points. The purple and blue probabilities listed for the 112 cm sample are the 2$\sigma$ values for the 0 and 15% marine calibrations, respectively (see Supplementary Table S1). The red and orange dashed lines represent the age models used in Fig. 4a.

The most arid conditions as demonstrated by the saltiest lake water (Fig. 4a) and most salt-tolerant microbes (Fig. 2e,f) occurred during the LIA from about AD 1420 to 1560/1640. Sometime between AD 1560/1640 and AD 1798, when the island was described as similar to today by the explorer Edmund Fanning[16], the climate and ecosystem of Washington Island was transformed into a tropical rainforest. We cannot rule out the possibility that arid conditions persisted well into the eighteenth century if the most recently deposited microbial mat sediment (that is, the top of Unit IIa) was destroyed by macrofauna and fish such as those that inhabit the lake today.

## Evidence from the west Pacific warm pool

Further evidence of a large hydrologic change in the tropical Pacific in the late eighteenth century comes from Palau in the west Pacific warm pool. The physical geography of the limestone islands permits seawater seepage into dozens of marine meromictic lakes that are highly stratified owing to the 3,730 mm rain they receive annually[23] (Fig. 1). The water chemistry and ecosystems of the lakes show little variation throughout the year[24] and their sediments are rich in plant detritus from the surrounding jungle. Permanent anoxia in the subsurface water confines phytoplankton, dominated by dinoflagellates and diatoms[24], to the oxygenated, brackish and deuterium-depleted surface water where their lipid $\delta$D values can be expected to closely co-vary with the surface water $\delta$Dvalues[25,26]. $\delta$D values of that water are controlled by the amount of rainfall, its isotopic composition and the amount of mixing with the underlying sea water. As rain also increases the density stratification in the lakes, decreasing mixing, surface water $\delta$D values are expected to be significantly lower during wet periods compared with dry periods. $\delta$D values of dinosterol, a lipid unique to dinoflagellate algae[27], that were extracted from the upper 63 cm of Spooky Lake

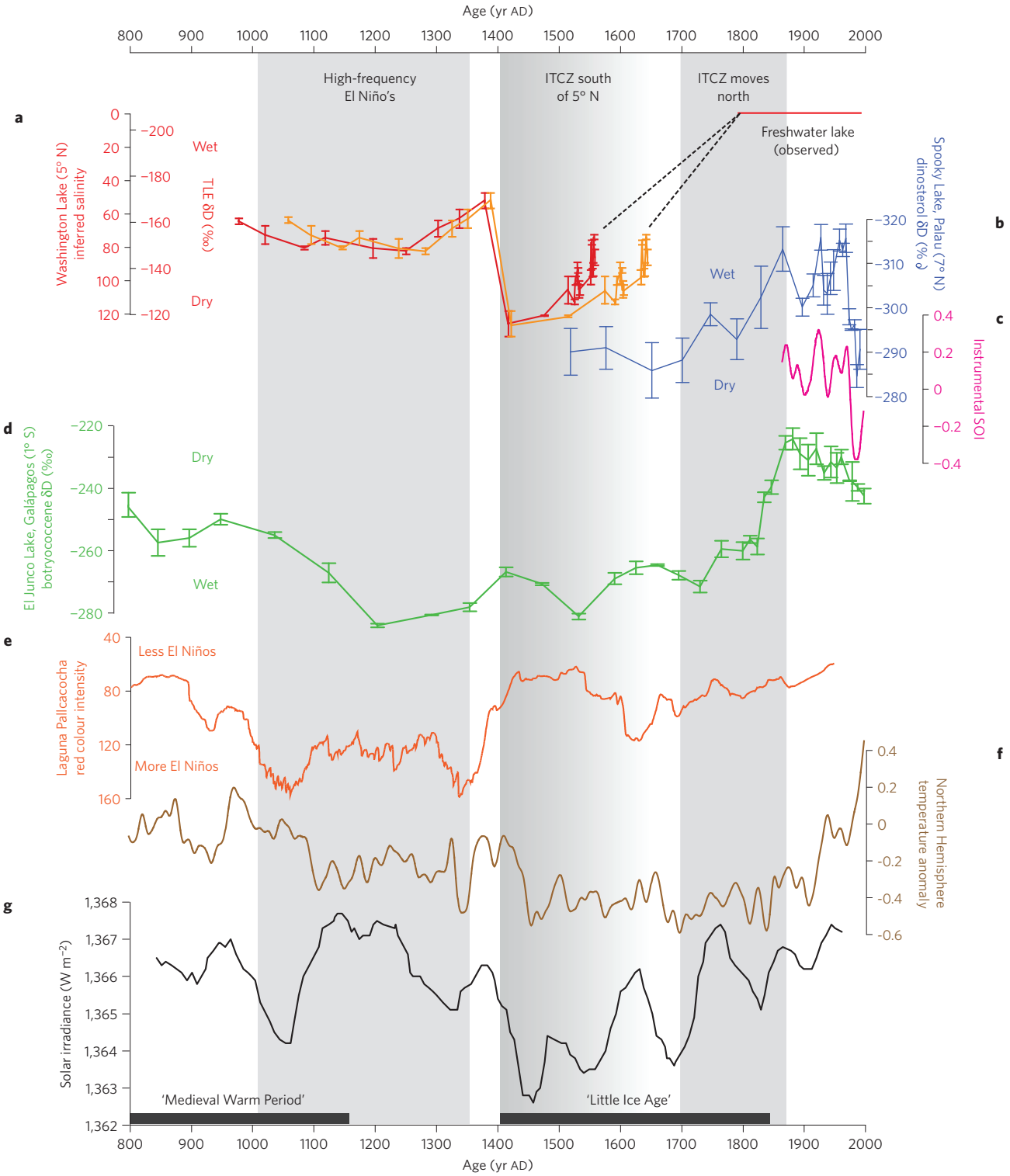


**Figure 4 | Tropical Pacific precipitation proxy records during the past 1,200 years and selected records from the literature. a**, Washington Island lake TLE $\delta$D values and inferred salinity[20]. The red and orange curves are based on two possible age models (red: atmospheric, orange: 15% marine) (Fig. 3). **b**, Palau Spooky Lake dinosterol $\delta$D values (blue). **c**, SOI (30 year Gaussian filter) based on instrumental data[45] (pink). **d**, Galápagos El Junco Lake botryococcene $\delta$D values (green). **e**, Andean Lake Pallcacocha red colour intensity, a proxy for El Niño frequency[32] (orange). **f**, Northern Hemisphere temperature reconstruction (land + ocean, 10 year smoothed)[1] (brown). **g**, Solar irradiance based on cosmogenic nuclides[36] (black). The error bars in **a**, **b** and **d** are standard deviations based on replicate isotopic measurements (see Supplementary Tables S5–S7). The grey shading from AD 980–1350 indicates high El Niño frequency (**e**), probably contributing to wet conditions in the Galápagos (**d**). The gradual grey shading from AD 1420–1640 indicates when Washington Island was driest (**a**) and the Northern Hemisphere was coldest (**f**), and most likely when the ITCZ was perennially south of 5° N. The grey shading from AD 1700–1870 indicates when Palau became substantially wetter (**b**), Galápagos became substantially dryer (**d**) and Washington Lake became fresh, all associated with the northward migration of the Pacific ITCZ to near its modern position centred on about 7° N, and the onset of post-LIA warming of the Northern Hemisphere.

(0.0125 km$^2$, 7°09′ N, 134°22′ E; 12 m deep) sediment correlate with the Southern Oscillation Index (SOI) over the past century, indicating that they reflect the regional climate (see Supplementary Discussion, Fig. S1).

In June 2004, Spooky Lake surface water (0–2.5 m) $\delta$D values were −17 to −19‰ and salinity was 20 psu, reflecting a mixture between rain water, with $\delta D = -45 \pm 28$‰ ($n = 6$) and salinity of 0 psu, and subsurface water (2.5–12 m), with $\delta D = -5.4 \pm 0.1$‰ ($n = 7$) and salinity of 29 psu. $\delta$D values of dinosterol that averaged $-291 \pm 4$‰ from about AD 1520 to 1795 were substantially higher than from AD 1830 to 1970 when they averaged $-309 \pm 6$‰ (Fig. 4b, Supplementary Tables S2 and S6). We attribute the 18‰ deuterium enrichment of dinosterol from AD 1520 to 1795 to less rain compared with the AD 1830–1970 period. Diminished rainfall is expected to increase dinosterol $\delta$D values through the additive effects of three mechanisms: (1) the amount effect (that is, the inverse correlation between the amount of rain and its isotopic composition) that would increase surface water $\delta$D values[28], (2) increased mixing of D-depleted surface water with D-enriched subsurface sea water as the density difference declined and (3) to the extent that it occurs in brackish water, diminished D/H fractionation during dinosterol synthesis in saltier surface water[20] (see Supplementary Discussion). High dinosterol $\delta$D values are again observed after 1970 when strong El Niño events in 1972, 1982, 1991 and 1997 caused droughts in Palau (for example, compare late twentieth century dinosterol $\delta$D values in Fig. 4b to SOI values in Fig. 4c).

## Evidence from the east Pacific cold tongue

Dry conditions in Palau and Washington Island during the LIA suggest that the ITCZ was located south of its modern position. To test that hypothesis, we reconstructed rainfall variations during the past 1,200 years at a site in the Galápagos Islands that lies south of the modern ITCZ throughout the year (Fig. 1). El Junco Lake (0°54′ S, 89°29′ W) on San Cristóbal Island is a freshwater lake that occupies an explosion crater at 760 m and is fed only by rain falling within the narrow crater rim. The lake level fluctuates by 50% or more, rising with El Niño rains and falling during La Niña droughts[29]. Unlike Spooky and Washington lakes, El Junco Lake is presumed to have remained fresh and therefore its lake-water $\delta$D value is dictated solely by the isotopic composition of precipitation, and the relative rates of evaporation and precipitation. More negative (positive) lake-water $\delta$D values reflect a greater (lesser) rate of rainfall relative to evaporation during wet (dry) periods.

El Junco sediments contained high concentrations of botryococcenes[30], lipids unique to the B race of the green alga *Botryococcus braunii*[31] for which the $\delta$D values have been shown to closely track water $\delta$D values[26]. Beginning at the end of the Medieval Warm Period (MWP) and extending through the LIA (about AD 1130–1830, Supplementary Tables S3 and S4), botryococcene $\delta$D values were low, averaging $-266 \pm 7$‰ ($n = 15$), before rising 33‰ from about AD 1830 to 1870 and remaining high through the twentieth century, averaging $-232 \pm 6$‰ ($n = 13$) from about AD 1870 to 2001 (Fig. 4d, Supplementary Table S7). During much of the MWP, botryococcene $\delta$D values were intermediate between those of the AD 1130–1830 and the AD 1870–2001 periods, averaging $-252 \pm 5$‰ ($n = 5$) from about AD 800 to 1040 (Fig. 4d, Supplementary Table S7). Relative to AD 1870–2001, botryococcene $\delta$D values were on average 34‰ and 20‰ lower during AD 1130–1830 and AD 800–1040, respectively. This indicates that the Galápagos were wetter during the LIA, and the 270 years that preceded it, than they were during the twentieth century and most of the MWP.

The low botryococcene $\delta$D values that preceded the LIA for about 270 years, reaching their lowest value about AD 1210, may have resulted at least in part from a 300 yr period when El Niño frequency is inferred by Moy *et al.* to have been substantially higher than at any time in the past 1,200 years[32] (Fig. 4e). El Niño events in the Galápagos are associated with torrential rains. As Washington Island also receives substantially higher than average rainfall during El Niño events[17], it may have been wetter, and Washington Lake may have been fresher, from about AD 980/1050 to 1405 (Fig. 4a) than they might otherwise have been if El Niño frequencies had not been elevated.

## Near-Equator position of Pacific ITCZ during the LIA

The observations of dry climates on Washington Island and in Palau and a wet climate in the Galápagos between about AD 1420–1560/1640 provide strong evidence for an ITCZ located perennially south of Washington Island (5° N) during that time and perhaps until the end of the eighteenth century, the last time Spooky Lake in Palau and El Junco Lake in the Galápagos had LIA-type $\delta$D values (Fig. 4a,b,d). The southern-most position of the ITCZ during the past millennium probably occurred about AD 1420, when the transition to extremely salt-tolerant microbes and the highest salinity since AD 980/1050 occurred in Washington Lake (Figs 2 and 4a). If Washington Island were just to the north of the boreal summer ITCZ, and the seasonal range of the ITCZ were comparable to the 7° range observed today (that is, 3°–10° N in boreal winter and summer, respectively), then it would have extended southward to at least the Equator, making the Galápagos humid. The near-Equator position of the ITCZ during the LIA was apparently short-lived. Soon after AD 1800, lipid $\delta$D values indicate that Palau transitioned to a substantially wetter climate (Fig. 4b) and the Galápagos to a substantially dryer climate (Fig. 4d), both supporting a northward retrenchment of the ITCZ.

An ITCZ located closer to the Equator during the LIA has been inferred previously from several studies on and near continental Asia[3,4,14], Africa[5–8], South[9,10], Central[11,12] and North[13] America. Our data complement these records while providing a constraint from the middle of the Pacific Ocean, where the ITCZ is unambiguous and meteorologically well defined, that the Pacific ITCZ was south of Washington Island, or 5° N, from about AD 1420–1560/1640.

At present there is no widely accepted theory to explain the position of the ITCZ, but a southward shift has been shown to occur in models when the cross-equatorial SST gradient is diminished[33], either by warming the eastern equatorial cold tongue[34], as occurs during El Niño events, or cooling the Northern Hemisphere extratropics[35], as occurred during the LIA. One possible scenario is that lower-than-modern solar irradiance during the LIA (ref. 36; Fig. 4g) may have provided the forcing to cool the Northern Hemisphere[37], which in turn drove the ITCZ close to the Equator[35]. AD 1420 in particular, when Washington Lake salinities were highest (Fig. 4a), corresponds to the minimum solar irradiance (Fig. 4g; the so-called Spörer Minimum)[36] and, except for a brief temperature minimum at about AD 1700, the coldest Northern Hemisphere temperatures (Fig. 4f) of the past 1,200 years[1].

Regardless of the mechanism, a 5° change in the position of the ITCZ during the past 400 years implies that the location of the tropical rain belt is either very sensitive to a change in radiative forcing as small as ~0.75 W m$^{-2}$ (that is, the surface equivalent of a 4 W m$^{-2}$ change in irradiance at the top of the atmosphere) or that its meridional position can change owing to natural phenomena on decadal-to-centennial timescales, perhaps associated with extratropical processes that help maintain the tropical thermocline. In either case, it suggests that increasing greenhouse gases could potentially shift the primary band of precipitation in the tropics with profound implications for the societies and economies that depend on it.

## Methods

**Sediment sampling.** Intact sediment–water interface cores (WL: Washington Lake, SL: Spooky Lake, EJ: El Junco Lake, CI: Christmas Island) were recovered with an adapted Livingstone-type piston corer and subsampled on site in 1 cm intervals and frozen the same day. Longer cores were taken with a Livingstone-type

piston corer (WL) or a Nesje corer (EJ), then split, imaged and subsampled in the laboratory. Further sampling details (such as for the CI microbial mats) are in Supplementary Information.

**Dating.** Depth–age models for SL and EJ were constructed on the basis of $^{210}$Pb and $^{14}$C radiogenic isotopes. The upper parts were constrained by radiocarbon analyses that indicated the presence or absence of nuclear-bomb-test-derived $^{14}$C, assumed to correspond to the early 1960s (see Supplementary Tables S2–S4). Materials used for radiocarbon dating of both lakes are not influenced by reservoir effects (see Supplementary Methods).

The WL sediment chronology was constructed from $^{14}$C dates of bulk organic matter, a terrestrial macrofossil and organic fractions from carbonate-containing samples (see Supplementary Table S1). Two age–depth models for core WL2 (units II–III) (Fig. 3) were constructed on the basis of four microbial sediment samples and one plant macrofossil at 571 cm, using the P_Sequence algorithm in the OxCal 4.0.1 beta software[38] with $k = 0.1\ \mathrm{cm}^{-1}$. One age model was constructed on the basis of calendar ages derived by use of the atmospheric calibration curve (lake-water bicarbonate in equilibrium with atmospheric $CO_2$) and the second by use of a mixed atmospheric–marine calibration curve that assumed a $15 \pm 5\%$ contribution of marine bicarbonate with a reservoir age of 314 yr (ref. 39). Several lines of evidence suggest little or no reservoir effect. (1) No authigenic mineral precipitates were observed within the microbial mat sedimentary units (unlike on Christmas Island[17]), indicating little or no intrusion of sea water and its pre-aged carbon. (2) Persistent hypersaline conditions indicate that the lake must have been disconnected from the sea most of the time, allowing equilibration with atmospheric $CO_2$. (3) The age of the uppermost microbial mat sediment (112 cm) pre-dates AD 1798, which is possible only when using a mixed calibration curve with less than 20% marine carbon (Fig. 3). (4) Even on Christmas Island where the environment is presumably very similar to Washington Lake during Unit II deposition but with some carbonate precipitates, modern radiocarbon contents in the top sediments (see Supplementary Table S1) suggest either no dissolution from the surrounding ancient coral or such reservoir effects are offset by the intrusion of sea water containing bomb-radiocarbon. Yet as the intrusion of some sea water cannot be ruled out in WL, we present both the 0% and 15% marine carbon age models, resulting in two possible ages for WL sediments.

**Microscopy.** Permanent slides were prepared approximately every 10 cm throughout the upper 571 cm of core WL2 and in the 70 cm core from lake F6 (CI). An Axioimager A1 microscope and Axiocam MRc imaging system and software (Carl Zeiss GmbH), or a Leica S6D microscope and a Canon G6 digital camera, were used for microscopy. Microbial morphotypes were identified in accordance with traditional phycological determination manuals[40–42].

**Lipid extraction and δD analysis.** Hydrogen isotope analysis of total lipid extracts from microbial mats (CI) and sediments (WL, CI) is described in ref. 20. Lipid extraction, purification and compound-specific hydrogen isotope analysis of botryococcenes (EJ) and dinosterol (SL) are described in refs 26, 30, 43.

The empirical relationship between TLE δD values and salinity in contemporary microbial mats and surface sediments on Christmas Island is $\delta D_{TLE} = 0.72 \cdot \text{salinity (in psu)} - 207‰$ ($r^2 = 0.70$, $n = 32$; ref. 20). This equation was used to estimate salinities from TLEs in Unit II–III sediments from Washington Island.

Supplementary Information contains: Supplementary Methods; Discussion of the influences on δD values of microbial sediment TLEs; Discussion about the use of dinosterol δD values from Spooky Lake and the correlation with the SOI; Data used in this study.

Received 20 February 2009; accepted 27 May 2009; published online 28 June 2009

## References


1. Mann, M. E. *et al.* Proxy-based reconstructions of hemispheric and global surface temperature variations over the past two millennia. *Proc. Natl Acad. Sci. USA* **105**, 13252–13257 (2008).
2. Trenberth, K. E. *et al.* Progress during TOGA in understanding and modeling global teleconnections associated with tropical sea surface temperatures. *J. Geophys. Res.* **103**, 14291–14324 (1998).
3. Newton, A., Thunell, R. & Stott, L. Climate and hydrographic variability in the Indo-Pacific Warm Pool during the last millennium. *Geophys. Res. Lett.* **33**, L19710 (2006).
4. Langton, S. J. *et al.* 3,500 yr record of centennial-scale climate variability from the Western Pacific Warm Pool. *Geology* **36**, 795–798 (2008).
5. Verschuren, D., Laird, K. R. & Cumming, B. F. Rainfall and drought in equatorial east Africa during the past 1,100 years. *Nature* **403**, 410–414 (2000).
6. Anderson, D. M., Overpeck, J. T. & Gupta, A. K. Increase in the Asian southwest monsoon during the past four centuries. *Science* **297**, 596–599 (2002).
7. Alin, S. R. & Cohen, A. S. Lake-level history of Lake Tanganyika, East Africa, for the past 2,500 years based on ostracode-inferred water-depth reconstruction. *Palaeogeogr. Palaeoclimatol. Palaeoecol.* **199**, 31–49 (2003).
8. Brown, E. T. & Johnson, T. C. Coherence between tropical East African and South American records of the Little Ice Age. *Geochem. Geophys. Geosys.* **6**, Q12005 (2005).
9. Haug, G. H. *et al.* Southward migration of the intertropical convergence zone through the Holocene. *Science* **293**, 1304–1308 (2001).
10. Sifeddine, A. *et al.* Laminated sediments from the central Peruvian continental slope: A 500 year record of upwelling system productivity, terrestrial runoff and redox conditions. *Prog. Oceanogr.* **79**, 190–197 (2008).
11. Linsley, B. K., Dunbar, R. B., Wellington, G. M. & Mucciarone, D. A. A coral-based reconstruction of intertropical convergence zone variability over Central America since 1707. *J. Geophys. Res.* **99**, 9977–9994 (1994).
12. Hodell, D. A. *et al.* Climate change on the Yucatan Peninsula during the Little Ice Age. *Quat. Res.* **63**, 109–121 (2005).
13. Lund, D. C., Lynch-Stieglitz, J. & Curry, W. B. Gulf Stream density structure and transport during the past millennium. *Nature* **444**, 601–604 (2006).
14. Zhang, P. *et al.* A test of climate, sun, and culture relationships from an 1810-year Chinese cave record. *Science* **322**, 940–942 (2008).
15. Chiang, J. C. H., Zebiak, S. E. & Cane, M. A. Relative roles of elevated heating and surface temperature gradients in driving anomalous surface winds over tropical oceans. *J. Atmos. Sci.* **58**, 1371–1394 (2001).
16. Wester, L., Juvik, J. & Holthu, P. Vegetation history of Washington Island (Teraina), Northern Line Islands. *Atoll Res. Bull.* **358**, 1–50 (1992).
17. Saenger, C., Miller, M., Smittenberg, R. & Sachs, J. A physico-chemical survey of inland lakes and saline ponds: Christmas Island (Kiritimati) and Washington (Teraina) Islands, Republic of Kiribati. *Sal. Syst.* **2**, 8 (2006).
18. Bauld, J. Occurrence of benthic microbial mats in saline lakes. *Hydrobiology* **81–82**, 87–111 (1981).
19. Fenchel, T. Formation of laminated cyanobacterial mats in the absence of benthic fauna. *Aquat. Microb. Ecol.* **14**, 235–240 (1998).
20. Sachse, D. & Sachs, J. P. Inverse relationship between D/H fractionation in cyanobacterial lipids and salinity in Christmas Island saline ponds. *Geochim. Cosmochim. Acta* **72**, 793–806 (2008).
21. Gonfiantini, R. *Handbook of Environmental Isotope Geochemistry* (Elsevier, 1986).
22. Garcia-Pichel, F., Nubel, U. & Muyzer, G.. The phylogeny of unicellular, extremely halotolerant cyanobacteria. *Arch. Microbiol.* **169**, 469–482 (1998).
23. Hamner, W. M. & Hamner, P. P. Stratified marine lakes of Palau (Western Caroline Islands). *Phys. Geogr.* **19**, 175–220 (1998).
24. Hamner, W. M., Gilmer, R. W. & Hamner, P. P. The physical, chemical, and biological characteristics of a stratified, saline, sulfide lake in Palau. *Limnol. Oceanogr.* **27**, 896–909 (1982).
25. Sessions, A. L., Burgoyne, T. W., Schimmelmann, A. & Hayes, J. M. Fractionation of hydrogen isotopes in lipid biosynthesis. *Org. Geochem.* **30**, 1193–1200 (1999).
26. Zhang, Z. & Sachs, J. P. Hydrogen isotope fractionation in freshwater algae: I. Variations among lipids and species. *Org. Geochem.* **38**, 582–608 (2007).
27. Volkman, J. K. *et al.* Microalgal biomarkers: A review of recent research developments. *Org. Geochem.* **29**, 1163–1179 (1998).
28. Gat, J. R. Oxygen and hydrogen isotopes in the hydrologic cycle. *Annu. Rev. Earth Planet. Sci.* **24**, 225–262 (1996).
29. Colinvaux, P. A. Climate and the Galápagos Islands. *Nature* **240**, 17–20 (1972).
30. Zhang, Z., Metzger, P. & Sachs, J. P. Biomarker evidence for the co-occurrence of three races (A, B and L) of *Botryococcus braunii* in El Junco Lake, Galápagos. *Org. Geochem.* **38**, 1459–1478 (2007).
31. Metzger, P., Berkaloff, C., Casadevall, E. & Coute, A. Alkadiene- and botryococcene-producing races of wild strains of *Botryococcus braunii*. *Phytochemistry* **24**, 2305–2312 (1985).
32. Moy, C. M., Seltzer, G. O., Rodbell, D. T. & Anderson, D. M. Variability of El Nino/Southern Oscillation activity at millennial timescales during the Holocene epoch. *Nature* **420**, 162–165 (2002).
33. Chiang, J. C. H., Cheng, W. & Bitz, C. M. Teleconnection mechanisms to the tropical Atlantic from an abrupt freshening of the North Atlantic Ocean. *Geophys. Res. Lett.* **35**, L07704 (2008).
34. Takahashi, K. & Battisti, D. S. Processes controlling the mean tropical Pacific precipitation pattern. Part I: The Andes and the eastern Pacific ITCZ. *J. Clim.* **20**, 3434–3451 (2007).
35. Chiang, J. C. H. & Bitz, C. M. Influence of high latitude ice cover on the marine Intertropical Convergence Zone. *Clim. Dyn.* **25**, 477–496 (2005).
36. Bard, E., Raisbeck, G., Yiou, F. & Jouzel, J. Solar irradiance during the last 1200 years based on cosmogenic nuclides. *Tellus B* **52**, 985–992 (2000).
37. Shindell, D. T., Schmidt, G. A., Miller, R. L. & Mann, M. E. Volcanic and solar forcing of climate change during the preindustrial era. *J. Clim.* **16**, 4094–4107 (2003).
38. Ramsey, C. B. Deposition models for chronological records. *Quat. Sci. Rev.* **27**, 42–60 (2008).
39. Druffel, E. R. M. Bomb radiocarbon in the Pacific: Annual and seasonal timescale variations. *J. Mar. Res.* **45**, 667–698 (1987).
40. Geitler, L. *Rabenhorst's Kryptogamenflora von Deutschland, Österreich und der Schweiz: 14 (1985 reprint: Königstein, Koletz Scientific Books)* (Akademische, 1932).

41. Komárek, J. & Anagnostidis, K. *Süßwasserflora von Mitteleuropa* (Gustav Fischer, 1999).
42. Komárek, J. & Anagnostidis, K. *Süßwasserflora von Mitteleuropa* (Gustav Fischer, 2005).
43. Smittenberg, R. H. & Sachs, J. P. Purification of dinosterol for hydrogen isotopic analysis using high-performance liquid chromatography–mass spectrometry. *J. Chromatogr. A.* **1169**, 70–76 (2007).
44. Wallace, J. M., Mitchell, T. P. & Lau, A. K.-H. Legates/MSU precipitation climatology, <http://jisao.washington.edu/legates_msu/> (1995).
45. Jones, P. D. & Mann, M. E. Climate over past millennia. *Rev. Geophys.* **42**, RG2002 (2004).

## Acknowledgements

Financial support was provided by the US National Science Foundation (J.P.S.), the US National Oceanic and Atmospheric Administration (J.P.S.), the Gary Comer Science and Education Foundation (J.P.S.) and the Alexander-von-Humboldt foundation through a Feodor-Lynen Research Fellowship (D.S.). Discussions with J. Chiang, K. Takahashi, A. Timmerman, M. Wallace, G. Philander, C. Wunsch, P. Colinvaux and C. Saenger improved this manuscript. M. Miller, C. Saenger, M. Dawson, L. Martin, P. Colin, L. Bell, The Coral Reef Research Foundation of Palau, J. Overpeck, J. Conroy, P. Colinvaux, M. Steinitz-Kannan, S. Fukada, K. Anderson, J. Briden and C. Corbett assisted with field work. O. Kawka, B. Demianew and R. Rottenfusser assisted in the laboratory. The Galápagos National Park, the Charles Darwin Foundation, the Republic of Kiribati and the Republic of Palau issued permits and provided assistance with field work.

## Author contributions

J.P.S. conceived the research, acquired financial support, carried out field work and wrote the paper. D.S. contributed the Line Island data, aided by S.G., and assisted with writing. Z.Z. contributed the El Junco data and assisted with writing. R.H.S. carried out field work, contributed the Palau data and assisted with writing. D.S.B. assisted with writing.

## Additional information

Supplementary information accompanies this paper on www.nature.com/naturegeoscience. Reprints and permissions information is available online at http://npg.nature.com/reprintsandpermissions. Correspondence and requests for materials should be addressed to J.P.S.